Electrostatic and Aromatic Microdomains within the Binding-Site Crevice of the D2 Receptor: Contributions of the Second Membrane-Spanning Segment†

Jonathan A. Javitch,*,‡,§ Juan A. Ballesteros,|| Jiayun Chen,‡ Victor Chiappa,‡ and Merrill M. Simpson‡

Center for Molecular Recognition and Departments of Psychiatry and Pharmacology, College of Physicians and Surgeons, Columbia University, 630 West 168th Street, New York, New York 10032, and Department of Physiology and Biophysics, Mount Sinai School of Medicine, New York, New York 10029

Received March 8, 1999; Revised Manuscript Received April 30, 1999

ABSTRACT: The binding-site of the dopamine D2 receptor, like that of other homologous G protein-coupled receptors, is contained within a water-accessible crevice formed among its seven membrane-spanning segments. Using the substituted cysteine accessibility method (SCAM), we previously mapped the residues in the third, fifth, sixth, and seventh membrane-spanning segments that contribute to the surface of this binding-site crevice. We have now mutated to cysteine, one at a time, 22 consecutive residues in the second membrane-spanning segment (M2) and expressed the mutant receptors in HEK 293 cells. Eleven of these mutants reacted with charged, hydrophilic, lipophobic, sulfhydryl-specific reagents, added extracellularly, and 9 of these 11 were protected from reaction by a reversible dopamine antagonist, sulpiride. We infer that the side chains of the residues at the 11 reactive loci (D80, L81, V83, V87, P89, W90, V91, V92, L94, E95, V96) are on the water-accessible surface of the binding-site crevice and that 9 of these are occluded by bound antagonist. The pattern of accessibility suggests an α-helical conformation. A broadening of the angle of accessibility near the binding site is consistent with the presence of a kink at Pro89. On the basis of the enhanced rates of reaction of positively charged sulfhydryl reagents, we infer the presence of an electrostatic microdomain composed of three acidic residues in M2 and the adjacent M3 that could attract and orient cationic ligands. Furthermore, based on the enhanced reactivity of the hydrophobic cation-containing reagent, we infer the presence of an aromatic microdomain formed between M2, M3, and M7.

The dopamine receptors, like the homologous receptors for the other biogenic amines, bind neurotransmitters present in the extracellular medium and couple this binding to the activation of intracellular G-proteins (*1*, *2*). The binding sites of these receptors are formed among their seven, mostly hydrophobic, membrane-spanning segments (*2*, *3*) and are accessible to charged, water-soluble agonists, like dopamine. Thus, for each of these receptors, the binding site is contained within a water-accessible crevice, the binding-site crevice, extending from the extracellular surface of the receptor into the transmembrane domain. The surface of this crevice is formed by residues that can contact specific agonists and/or antagonists and by other residues that may play a structural role and affect binding indirectly.

To identify the residues that form the surface of the binding-site crevice in the human D2 receptor, we have used the substituted-cysteine accessibility method (SCAM)[1] (*4*−*10*). Consecutive residues in the membrane-spanning segments are mutated to cysteine, one at a time, and the mutant receptors are expressed in heterologous cells. If ligand binding to a cysteine substitution mutant is near normal, we assume that the structure of the mutant receptor, especially around the binding site, is similar to that of wild-type and that the substituted cysteine lies in a similar orientation to that of the wild-type residue. In the membrane-spanning segments, the sulfhydryl of a cysteine facing into the binding-site crevice should react much faster with charged sulfhydryl-specific reagents than should sulfhydryls facing into the interior of the protein or into the lipid bilayer. For such reagents, we use derivatives of methanethiosulfonate (MTS): positively charged MTS ethylammonium (MTSEA) and MTS ethyltrimethylammonium (MTSET), and negatively charged MTS ethylsulfonate (MTSES) (*11*). These reagents are about the same size as dopamine, with maximum dimensions of approximately 10 Å by 6 Å. They form mixed disulfides with the cysteine sulfhydryl, covalently linking $-SCH_2CH_2X$, where X is NH_3^+, $N(CH_3)_3^+$, or SO_3^-. We use two criteria for identifying an engineered cysteine as forming the surface of the binding-site crevice: (i) the reaction with an MTS reagent alters binding irreversibly; (ii) this reaction is retarded by the presence of ligand.

† This work was supported in part by NIH Grants MH57324 and MH54137, by the G. Harold & Leila Y. Mathers Charitable Trust and by the Lebovitz Trust.

* To whom correspondence should be addressed, Columbia University, P&S 11-401, Box 7, 630 W. 168th St., New York, NY 10032. E-mail: jaj2@columbia.edu. Phone: 212-305-7308. Fax: 212-305-5594.

‡ Center for Molecular Recognition.

§ Departments of Psychiatry and Pharmacology.

|| Department of Physiology and Biophysics at Mt. Sinai.

[1] Abbreviations: SCAM, substituted-cysteine accessibility method; Mn, the *n*th membrane-spanning segment; MTS, methanethiosulfonate; MTSEA, MTS ethylammonium; MTSET, MTS ethyltrimethylammonium; MTSES, MTS ethylsulfonate; MMTS, methylmethanethiosulfonate; GPCRs, G-protein-coupled receptors; WT, wild-type.

10.1021/bi9905314 CCC: $18.00
Published on Web 06/03/1999

On the basis of site-directed mutagenesis experiments, a number of laboratories have implicated residues in the second membrane-spanning segment (M2) of G-protein-coupled receptors (GPCRs) in antagonist binding (*12*, *13*). Moreover, a reactive antagonist covalently labeled this region, although the specific residue labeled could not be identified (*14*). M2 contains the highly conserved Asp80, which has been implicated in Na^+ binding and in receptor activation (*15*, *16*), and this residue has been postulated to interact with a highly conserved Asn in M7 (*17*, *18*). Here, we report the application of SCAM to identify systematically all the residues in M2 of the D2 receptor that contribute to the binding-site crevice.

EXPERIMENTAL PROCEDURES

Numbering of Residues. Residues are numbered according to their positions in the human dopamine $D2_{Short}$ receptor sequence. In some cases, we also index residues relative to the most conserved residue in the membrane-spanning segment in which it is located (*19*). By definition, the most conserved residue is assigned the position index "50", e.g., $Asp80^{(2.50)}$, and therefore $Ala79^{(2.49)}$ and $Leu81^{(2.51)}$. This indexing simplifies the identification of corresponding residues in different GPCRs.

Site-Directed Mutagenesis. Cysteine mutations were generated as described previously (*7*). Mutations were confirmed by DNA sequencing. Mutants are named as (wild-type residue)(residue number)(mutant residue), where the residues are given in the single-letter code.

Transient and Stable Transfection. The cDNA encoding the dopamine $D2_S$ receptor or the appropriate cysteine mutant, epitope tagged at the amino terminus with the cleavable influenza-hemagglutinin signal sequence followed by the "FLAG"-epitope (IBI, New Haven, CT) (*10*) in the bicistronic expression vector pcin4 (a gift from Dr. S. Rees, Glaxo) (*20*), was used for all transfections, which were performed as described previously (*10*).

HEK 293 cells in DMEM/F12 (1:1) with 10% bovine calf serum (Hyclone) and 293-TSA cells (a clonal line of HEK 293 cells stably expressing the SV40 large T antigen) in DMEM with 10% fetal calf serum were maintained at 37 °C and 5% CO_2. For transient transfection, 35 mm dishes of 293-TSA cells at 70−80% confluence were transfected with 2 μg of wild-type or mutant D2 receptor cDNA in pcin4 (see above) using 9 μL of lipofectamine (Gibco) and 1 mL of OPTIMEM (Gibco). Five hours after transfection, the solution was removed and fresh media added. Twenty-four hours after transfection, the media was changed. Forty-eight hours after transfection, cells were harvested as described below. For stable transfection, HEK 293 cells were transfected with D2 receptor cDNA in pcin4 as described above. Twenty-four hours after transfection, the cells were split to a 100 mm dish and 700 μg/mL Geneticin was added to select for a stably transfected pool of cells.

Harvesting cells. Cells were washed with phosphate-buffered saline (PBS; 8.1 mM NaH_2PO_4, 1.5 mM KH_2PO_4, 138 mM NaCl, and 2.7 mM KCl, pH 7.2), briefly treated with PBS containing 1 mM EDTA, and then dissociated in PBS. Cells were pelleted at 1000*g* for 5 min at 4 °C and resuspended for binding or treatment with MTS reagents.

[^{3}H]N-Methylspiperone Binding. Whole cells from a 35 mm plate were suspended by pipetting in 400 μL of buffer A (25 mM Hepes, 140 mM NaCl, 5.4 mM KCl, 1 mM EDTA, and 0.006% BSA, pH 7.4). Cells were then diluted with buffer A, typically 20-fold. Depending on the level of expression in the various mutants, adjustments in the number of cells per assay tube were made as necessary to prevent depletion of ligand in the case of very high expression or to increase the signal in the case of low expression. [^{3}H]*N*-Methylspiperone (Dupont/NEN) binding was performed as described previously (*9*).

Reactions with MTS Reagents. Whole cells from a 35 mm plate were suspended in 400 μL of buffer A. Aliquots (45 μL) of cell suspension were incubated with freshly prepared MTS reagents (5 μL) at the stated concentrations at room temperature for 2 min. Cell suspensions were then diluted 16-fold, and 200 μL aliquots were used to assay for [^{3}H]*N*-methylspiperone (200 pM) binding as described (*9*). The fractional inhibition was calculated as 1 − [(specific binding after MTS reagent)/(specific binding without reagent)]. We used the SPSS for Windows (SPSS, Inc.) statistical software to analyze the effects of the MTS reagents by one-way ANOVA according to Dunnett's post hoc test ($p < 0.05$).

The second-order rate constant (k) for the reaction of MTSEA with each susceptible mutant was estimated by determining the extent of reaction after a fixed time, 2 min, with six concentrations of MTSEA (typically 0.025−10 mM) (all in excess over the reactive sulfhydryls). The fraction of initial binding, Y, was fit to $(1 - \text{plateau})e^{-kct} + \text{plateau}$, where plateau is the fraction of residual binding at saturating concentrations of MTSEA, k is the second-order rate constant (M^{-1} s^{-1}), c is the concentration of MTSEA (M), and t is the time (120 s).

RESULTS

Effects of Cysteine-Substitution on Antagonist Binding. In a background of the mutant C118S, which is relatively insensitive to the MTS reagents (*6*), we mutated to cysteine, one at a time, 22 consecutive residues, Ala77 to Gly98, in M2. Each mutant receptor was transiently or stably expressed in HEK 293 cells, and the K_D and B_{MAX} characterizing the equilibrium binding of the radiolabeled antagonist, [^{3}H]*N*-methylspiperone, were determined. At all 22 positions, the K_D of the cysteine substitution mutant was between 0.3 and 2.4 times the K_D of C118S (Table 1). For 21 of these mutants, B_{MAX} ranged from 33 to 250% of that obtained with C118S (Table 1). P89C expressed at only 5% of the level observed with C118S (Table 1).

The K_I of the antagonist sulpiride in competition with [^{3}H]-*N*-methylspiperone was determined in the 22 mutants (Table 2). At 20 positions, the K_I was between 0.4 and 1.3 times the K_I of C118S; in D80C and L81C, the K_I was 7 and 10 times the K_I of C118S.

Reactions of MTSEA with the Mutants. When statistical significance was defined by Dunnett's post hoc test, 2.5 mM MTSEA significantly inhibited [^{3}H]*N*-methylspiperone binding to 11 of 22 cysteine substitution mutants (Figure 1A). MTSEA at 0.25 mM significantly blocked binding to 4 of these 11 mutants (Figure 1B).

To quantitate the susceptibility to MTSEA, we determined the second-order rate constants for the reaction with MTSEA (Table 3). The most reactive cysteines were those substituted for Val83, Val91, Leu94, and Glu95. Cysteine substituted

Table 1: Characteristics of [^{3}H]*N*-methylspiperone Binding to Cysteine-Substituted Dopamine D2 Receptor[a]

mutant	K_D (pM)	K_{MUT}/K_{C118S}	B_{MAX} (fmol/cm^2)	n
C118S	79 ± 14	1.0	133 ± 11	5
A77C	63 ± 7	0.8	126 ± 36	2
V78C	112 ± 49	1.4	273 ± 50	2
A79C	74 ± 32	0.9	140 ± 28	2
D80C	28 ± 7	0.4	44 ± 8	2
L81C	106 ± 8	1.3	275 ± 4	2
L82C	70 ± 32	0.9	194 ± 138	2
V83C	70 ± 23	0.9	280 ± 128	2
A84C	54 ± 8	0.7	111 ± 35	2
T85C	55 ± 12	0.7	166 ± 27	2
L86C	71 ± 21	0.9	184 ± 79	2
V87C	22 ± 2	0.3	74 ± 1	2
M88C	68 ± 4	0.9	225 ± 6	2
P89C	114 ± 22	1.4	7 ± 1	2
W90C	83 ± 5	1.0	103 ± 36	2
V91C	191 ± 13	2.4	334 ± 68	4
V92C	53 ± 7	0.7	117 ± 33	2
Y93C	97 ± 17	1.2	207 ± 18	2
L94C	66 ± 9	0.8	153 ± 46	3
E95C	134 ± 11	1.7	185 ± 42	2
V96C	33 ± 0	0.4	86 ± 6	2
V97C	62 ± 8	0.8	210 ± 84	2
G98C	46 ± 3	0.6	147 ± 50	2

[a] Cells transfected with the appropriate receptor were assayed as described in the Experimental Procedures. Data were fit to the binding isotherm by nonlinear regression. The means and SEM are shown for *n* independent experiments, each with duplicate determinations. B_{MAX} values are presented as femtomoles per square centimeter of plate area.

Table 2: Inhibitory Potency of (−)Sulpiride on [^{3}H]*N*-methylspiperone Binding to Cysteine-Substituted Dopamine D2 Receptor[a]

mutant	apparent K_I (nM)	$K_{I(MUT)}/K_{I(C118S)}$	n
C118S	7 ± 3	1.0	2
A77C	7 ± 4	1.0	2
V78C	4 ± 2	0.6	2
A79C	5 ± 3	0.7	2
D80C	47 ± 18	7.0	2
L81C	69 ± 4	10.3	3
L82C	5 ± 0	0.8	3
V83C	4 ± 1	0.6	2
A84C	5 ± 1	0.8	2
T85C	5 ± 1	0.7	3
L86C	4 ± 2	0.6	2
V87C	3 ± 0	0.4	3
M88C	4 ± 0	0.7	2
P89C	8 ± 3	1.3	2
W90C	9 ± 0	1.3	2
V91C	4 ± 1	0.5	2
V92C	6 ± 1	0.9	2
Y93C	5 ± 1	0.8	2
L94C	4 ± 1	0.7	2
E95C	7 ± 0	1.1	2
V96C	3 ± 0	0.4	2
V97C	3 ± 1	0.5	2
G98C	2 ± 0	0.4	2

[a] Cells transfected with the appropriate receptor were assayed with [^{3}H]*N*-methylspiperone (150 pM) as described in the Experimental Procedures in the presence of nine concentrations of (−)-sulpiride. The apparent K_I was determined by the method of Cheng and Prusoff (40) using the IC_{50} value obtained by fitting the data to a one site competition model by nonlinear regression. The means and SEM are shown for *n* independent experiments, each with duplicate determinations.

for Pro89 was of intermediate reactivity with MTSEA. Cysteines substituted for Asp80, Leu81, Val87, Trp90, Val92, and Val96 were least reactive.

The reversible antagonist sulpiride significantly retarded the reaction of MTSEA with D80C, L81C, V83C, V87C, P89C, W90C, V91C, L94C, and E95C. (Protection could not reliably be determined with V92C and V96C due to the small effect of MTSEA.) The degree of protection varied from 17 to 94% (Figure 2).

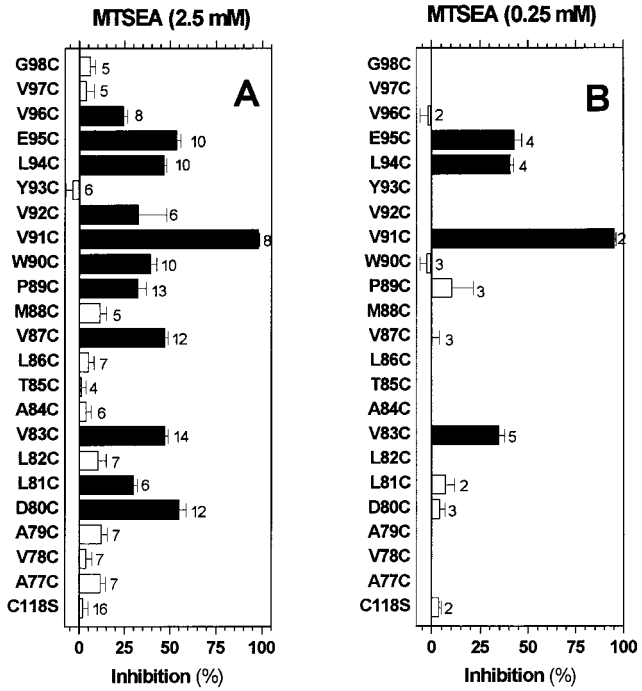

FIGURE 1: The inhibition of specific [^{3}H]*N*-methylspiperone (200 pM) binding to intact cells transfected with wild-type or mutant D2 receptors resulting from a 2-min application of (A) 2.5 mM MTSEA or (B) 0.25 mM MTSEA. The means and SEM are shown. The number of independent experiments for each mutant is shown next to the bars. Solid bars indicate mutants for which inhibition was significantly different ($p < 0.05$) than C118S by one-way ANOVA. Only the mutants that were significantly different from C118S at 2.5 mM MTSEA were studied at 0.25 mM in panel B.

Table 3: Rates of Reaction of MTSEA with Cysteine-Substituted Dopamine D2 Receptor[a]

mutant	k_{MTSEA} (M^{-1} s^{-1})	k_{MUT}/k_{WT}	*n*
D80C	4 ± 0	0.1	3
L81C	2 ± 0	0.1	2
V83C	49 ± 7	1.3	5
V87C	2 ± 1	0.1	3
P89C	17 ± 13	0.4	3
W90C	2 ± 0	0.1	3
V91C	290 ± 4	7.4	2
V92C	2 ± 1	0.1	2
L94C	169 ± 59	4.3	4
E95C	90 ± 19	2.3	4
V96C	2 ± 1	0.1	2

[a] The second-order rate constant (*k*) was determined as described in the Experimental Procedures. The means and SEM of *n* independent experiments, each performed with triplicate determinations, are shown. k_{MUT}/k_{WT} was obtained by dividing each *k* value by the *k* determined for the wild-type receptor in which Cys118 reacts, 39 M^{-1} s^{-1} (*7*).

Reactions with MTSET and MTSES. Only five of the mutants, P89C, V91C, V92C, L94C, and E95C were susceptible to reaction with 1mM MTSET (Figure 3A). At 10 mM, MTSES, the negatively charged derivative, significantly inhibited binding to P89C, V91C, and V92C and significantly potentiated binding to E95C (Figure 3B). Because we observed much greater inhibition of binding to V91C by MTSET than by MTSES, we determined the rates of reaction of these reagents with this mutant. The rates of

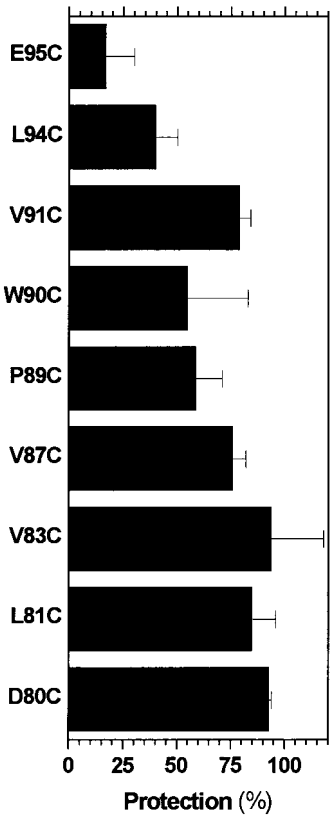

FIGURE 2: Sulpiride protection of cysteine substitution mutants. Dissociated cells were incubated in buffer A for 20 min at room temperature in the presence or absence of (±)-sulpiride and then MTSEA was added, in the continued presence or absence of sulpiride, for 2 min at a concentration chosen to inhibit 50−75% of specific binding in the absence of sulpiride. Concentrations of MTSEA were as follows: 2.5 mM, D80C, L81C, V87C, P89C, W90C; 1 mM, V83C; 0.25 mM or 0.1 mM, L94C, E95C; 0.025 mM, V91C. For most mutants, sulpiride was used at a concentration of 10 μM. To compensate for changes in the K_I, 50 and 100 μM sulpiride were used for D80C and L81C, respectively. Protection was calculated as 1-[(inhibition in the presence of sulpiride)/(inhibition in the absence of sulpiride)]. Protection by sulpiride was significant ($p < 0.05$) by paired *t*-test for all of the mutants.

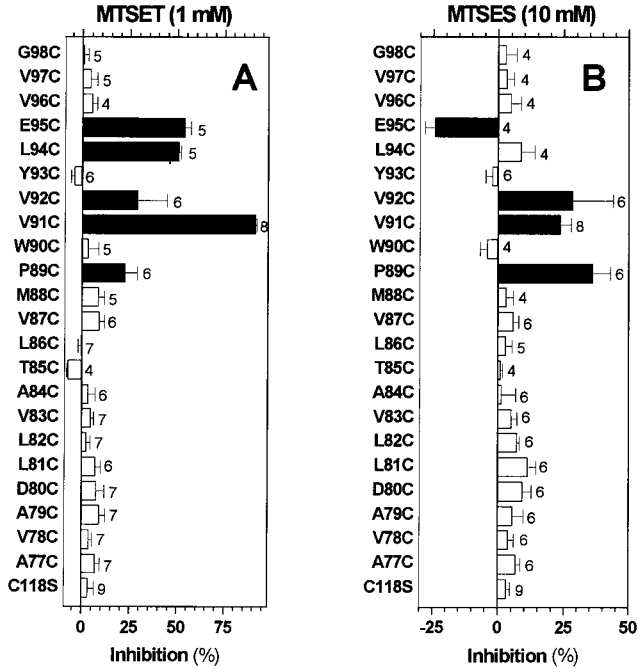

FIGURE 3: The inhibition of specific [^{3}H]*N*-methylspiperone (200 pM) binding to intact cells transfected with wild-type or mutant D2 receptors resulting from a 2-min application of (A) 1 mM MTSET or (B) 10 mM MTSES. On the basis of the relative rate constants for reaction with simple thiols in solution, namely 10:4:1 for MTSET, MTSEA, and MTSES, (*11*), we used equireactive concentrations of 1 mM MTSET (A), 2.5 mM MTSEA (Figure 1A), and 10 mM MTSES (B). The means and SEM are shown. The number of independent experiments for each mutant is shown next to the bars. Solid bars indicate mutants for which inhibition was significantly different ($p < 0.05$) than C118S by one-way ANOVA.

reaction of MTSET and of MTSES were 94.6 ± 2.7 M^{-1} s^{-1} ($n = 2$) and 0.8 ± 0.2 M^{-1} s^{-1} ($n = 2$), respectively. After normalizing by the ratio of the rate constants for their reactions with β-mercaptoethanol in solution (*11*), we found that the positively charged reagent reacted at V91C approximately 10-fold faster than did the negatively charged reagent.

DISCUSSION

Residues Forming the Water-Accessible Surface of the Binding-Site Crevice. We identify residues on the water-accessible surface of the D2 receptor by the ability of the MTS reagents to react with substituted cysteine residues. The MTS reagents react greater than 10^9 times faster with ionized thiolates than with un-ionized thiols (*21*), and only water-accessible cysteines are likely to ionize to a significant extent. Moreover, MTSEA, MTSET, and MTSES are charged and hydrophilic. Thus, we assume that these reagents will react much faster with water-accessible cysteine residues than with cysteines facing the protein interior or lipid. We infer that the MTS reagents have reacted if the binding of ligand is irreversibly affected. On the basis of the near-normal affinities of the cysteine mutants for ligand, it is likely that the global structures of the mutants are near normal and that the substituted cysteines are reliable reporters for the accessibility of the wild-type residue for which they are substituted. Thus, we infer that 11 of the 22 residues tested are on the water-accessible surface of the D2 receptor. These include 2 charged and 9 hydrophobic amino acids: Asp80$^{(2.50)}$, Leu81$^{(2.51)}$, Val83$^{(2.53)}$, Val87$^{(2.57)}$, Pro89$^{(2.59)}$, Trp90$^{(2.60)}$, Val91$^{(2.61)}$, Val92$^{(2.62)}$, Leu94$^{(2.64)}$, Glu85$^{(2.65)}$, and Val96$^{(2.66)}$ (Figure 1).

The residues that form the surface of the binding-site crevice are a subset of the water-accessible residues. We infer that water-accessible residues are in the binding-site crevice if competitive antagonists or agonists retard the reaction of the MTS reagents. The competitive antagonist sulpiride protected all of the residues tested[2], but the extent of protection by sulpiride varied considerably among the mutants (Figure 2). L94C and E95C are likely located at the extracellular margin of the binding site such that the presence of sulpiride in the binding site only partially decreases access of MTSEA, resulting in relatively poor protection of these mutants. Protection of a substituted cysteine is most simply explained by its proximity to the sulpiride-binding site. Nevertheless, not every one of these residues need contact sulpiride. Sulpiride could protect

[2] We were unable to test reliably for sulpiride protection with the mutants V92C and V96C because the inhibition by MTSEA was too small.

residues deeper in the crevice by binding above them and blocking the passage of MTSEA from the extracellular medium toward the cytoplasmic end of the crevice. We also cannot rule out indirect effects through propagated structural changes for protection by the antagonist sulpiride, although such changes are less likely caused by an antagonist than by an agonist.

A reactive derivative of a β2-adrenergic receptor antagonist was covalently incorporated into the second membrane-spanning segment of the β2 receptor (*22*). These authors speculated that Ser92$^{(2.63)}$ and/or His93$^{(2.64)}$ were the labeled residues. In the homologous D2 receptor, we found that Tyr93$^{(2.63)}$ was not accessible in the binding-site crevice, while Leu94$^{(2.64)}$ was accessible. These results support the aligned His93$^{(2.64)}$ as the labeled residue in the β2 adrenergic receptor. Moreover, Phe86$^{(2.64)}$, the aligned residue in the α1A adrenergic receptor, has been shown to be the critical determinant of the subtype selectivity of dihydropyridine antagonists (*13*), further supporting a functional role for this residue at the surface of the binding-site crevice. We also have recently determined that accessible residues in M2 of the dopamine D2 receptor are critical determinants of the pharmacological differences between the D2 and D4 receptors (Simpson et al., manuscript in preparation).

Secondary Structure of M2. The pattern of the residues which are accessible to the MTS reagents is consistent with M2 being α-helical, with a wider exposure for two helical turns near the binding site and a narrower stripe continuing toward the cytoplasm (Figure 4). A possible explanation for the broadening of exposure, which begins at Pro89, is the presence of a proline kink (*23*) at this position. Such a kink could bend the extracellular portion of M2 into the binding-site crevice where a wider arc would be exposed to water, an effect similar to that which we recently proposed for the conserved Pro in M6 of the D2 receptor (*10*). In contrast, the portion of M2 more cytoplasmic than the proline kink is either tightly packed against neighboring membrane-spanning segments or exposed to lipid, resulting in an accessibility to MTSEA restricted to a narrower stripe in this region. In this more tightly packed region, replacement of Leu81 by the smaller Cys may create a small cavity in the structure, which, along with the negative potential near Asp80 (see below), may increase the access of MTSEA to this substituted cysteine.

Highly conserved Pro residues are found in M2, M5, M6, and M7 of GPCRs and may play a crucial structural and functional role (*24*−*27*). In M7 of the D2 receptor, the pattern of accessibility of the cysteine substitution mutants was consistent with M7 being a kinked α-helix, but in this case, a significant face-twist at the kink was required to fit the experimental data (*9*). In M2 and in M6, the pattern of accessibility is straight and thus a simple bend and/or conformational flexibility at the Pro kink is sufficient to explain the data (*10*).

The reason for the significant reactivity of P89C is unclear. The helical wheel and net (Figure 4) demonstrate that the residues at the margin of the stripe of accessibility, namely Trp90 and Val96 react more slowly with MTSEA (Table 3) and do not react at all with the slightly larger MTSET or MTSES. Thus, these residues are likely to be at the margins of the binding-site crevice near the interface with M1 for Val 96 and with M3 for Trp90. Pro89 would be expected to

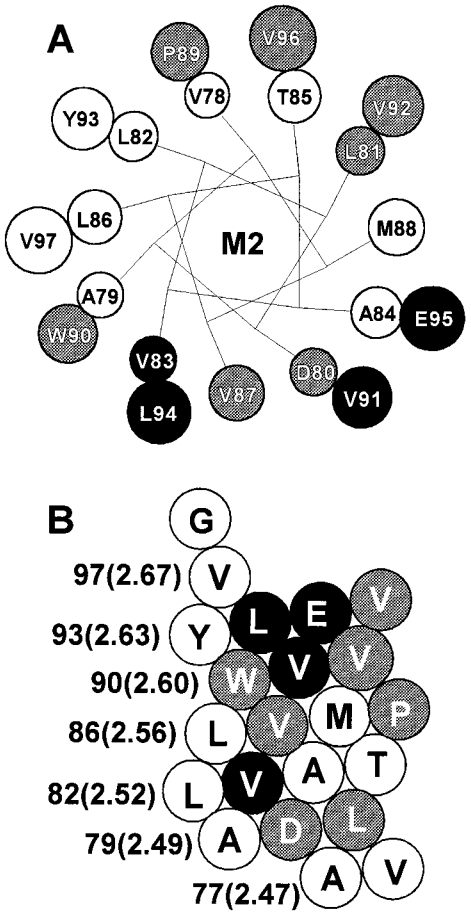

FIGURE 4: Helical wheel (A) and helical net (B) representations of the residues in and flanking the M2 segment of the dopamine D2 receptor, summarizing the effects of MTSEA on [^{3}H]*N*-methylspiperone binding. Reactive residues are solid filled for residues with rates of reaction $\geq$49 M^{-1} s^{-1} and shaded for residues that were significantly inhibited by MTSEA but had a rate $\leq$17 M^{-1} s^{-1}. Open circles indicate that MTSEA had no significant effect on binding. In panel A, increasing sizes of the circles indicate increasingly extracellular localization of the indicated residues.

be even more toward the interface with M1, but the reactivity of P89C with both MTSEA and with MTSET is significantly greater than with V92C or V96C. The explanation for this finding is not clear. While this mutant bound *N*-methylspiperone and sulpiride with near-normal affinity, its level of expression was only about 5% of C118S. Because of the significant role that prolines can play in kinking α-helices, it is possible that the structure of the P89C mutant is altered in such a way as to make the substituted-cysteine an imperfect reporter for the position of the wild-type Pro at this position.

None of the MTS reagents affected antagonist binding to V97C or G98C. Thus, these residues are probably not on the surface of the binding-site crevice, but rather in the loop from M1. The apparent inaccessibility of V97C would still be compatible with the α-helical pattern of accessibility for M2, but the apparent lack of accessibility of G98C breaks this pattern, thus defining the likely end of the M2 helix. With residues out of the membrane-spanning segments, however, the lack of an effect of the reagents is difficult to interpret. We have observed, in rare cases, that a residue forming the surface of the binding-site crevice can be covalently modified by the addition of the charged $-SCH_2-CH_2NH_3^+$ without interfering with binding of a particular

ligand (*28*). A lack of effect of chemical modification would be less surprising in a loop not directly involved with binding. It is also possible, either in a loop or in the membrane-spanning segment, for local steric factors to make a water-accessible residue inaccessible to the MTS reagents.

Electrostatic Potential in the Binding-Site Crevice. The relatively high rate of reaction of V91C with MTSEA likely results from the presence of Glu95, which attracts the ammonium moiety of MTSEA, thereby positioning the disulfide moiety of the reagent where it can be attacked by the thiolate of V91C (Figure 5A). A similar interaction with Glu95 likely contributes to the reactivity of MTSEA with V94C (not shown). Consistent with such an interpretation, the rate of reaction of V91C was more than 100-fold faster with the positively charged MTSET than with the negatively charged MTSES. After normalizing by the intrinsic reactivities of the reagents (*11*), reaction of V91C with MTSET was favored by approximately 10-fold over reaction with MTSES, consistent with a substantial negative electrostatic potential (*11*). Although we did not determine the rates of reaction at L94C, the greater extent of reaction seen with 1 mM MTSET than with 10 mM MTSES is consistent with a local negative electrostatic potential at this position as well.

It is also notable that the rate of reaction of MTSEA with V83C, relatively deep in the binding-site crevice, was greater than that seen at the more extracellular V87C. An electrostatic interaction between Asp80 and MTSEA may also explain the relatively high rate of reaction of V83C.

While reaction of E95C with the positively charged MTSEA and MTSET inhibited subsequent ligand binding, reaction of E95C with MTSES potentiated binding. Potentiation of binding by MTSES was also observed with D108C in M3 (*7*). In both cases, mutation of the acidic residue to cysteine slightly decreased the binding affinity of the radiolabeled antagonist. Reaction with MTSES covalently adds $-SCH_2CH_2SO_3^-$ to the cysteine. This restores a negative charge to the side chain, as found in WT, and increases the affinity of the receptor for ligand. In contrast, reaction of the positively charged reagents adds a positive charge to the side chain, further disrupting binding. Thus, the two negatively charged residues, Glu95 and Asp108, likely play an electrostatic role in ligand binding. Steric contributions of these residues appear to be less stringent than for Asp114, as D114C did not bind ligand even after treatment with MTSES (*7*).

There are only four acidic residues that are accessible in the binding-site crevice within the transmembrane domain of the D2 receptor: Asp80 and Glu95 in M2 and Asp108 and Asp114 in M3 (*7*−*10*). Current structural knowledge of related receptors allows an analysis of the relative spatial distribution of these four acidic groups. Electron cryomicroscopy studies of bovine rhodopsin have revealed the presence of seven helices in the transmembrane domain (*29*, *30*), and M2 and M3 have been proposed to be adjacent in the tertiary structure of the receptor (*31*). This inference has been further supported in the NK1 receptor by the spatial proximity inferred between $His^{(2.64)}$ and $His^{(3.28)}$, which form a Zn^{2+}-binding site (*32*). In the D2 receptor, these residues correspond to $Leu94^{(2.64)}$ in M2 and $Phe110^{(3.28)}$ in M3, and based on the structural similarity among these receptors these residues are also likely to be in proximity (Figure 5B). $Glu95^{(2.65)}$, which is adjacent to $Leu94^{(2.64)}$, is, therefore, likely

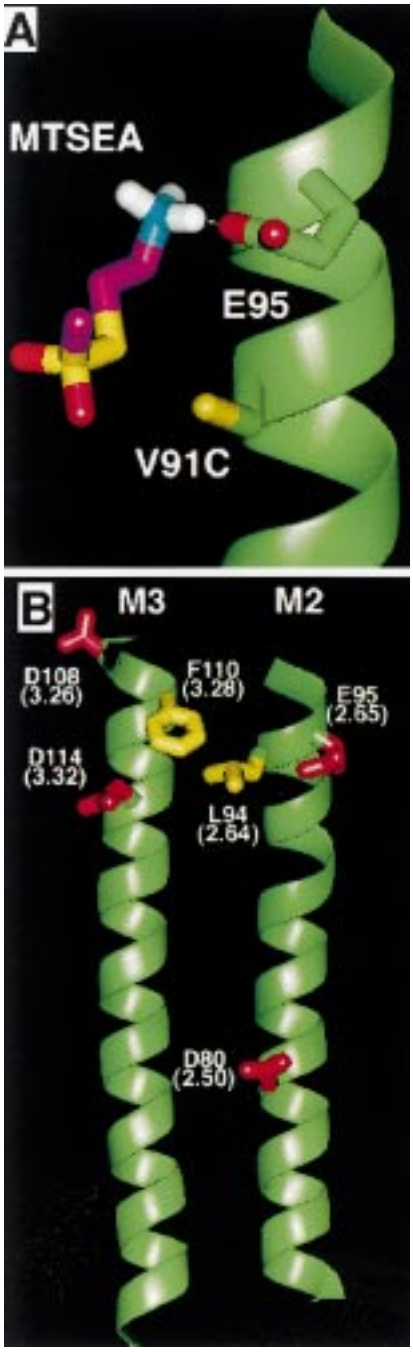

FIGURE 5: A negatively charged electrostatic microdomain in the binding-site crevice of the D2 receptor. (A) Molecular model of the interaction between M2 and MTSEA. The positively charged ammonium group of MTSEA is attracted to $E95^{(2.64)}$, orienting the disulfide of MTSEA in the right geometry for a nucleophilic attack by the thiolate of the substituted Cys at Val91. (B) The only four acidic residues (red) identified by SCAM as accessible in the binding-site crevice of the D2 receptor are located in M2 and M3, modeled here as adjacent α-helices (see text) viewed from the interior of the binding-site crevice. The axial displacement between these helices is dictated by the proximity between $Phe110^{(3.28)}$ in M3 and $Leu94^{(2.64)}$ in M2 shown in yellow, inferred from an engineered bis-His zinc binding site in the equivalent positions of the homologous NK1 receptor (*32*). Note that $Glu95^{(2.65)}$ in M2 is in the vicinity of $Asp108^{(3.26)}$ and $Asp114^{(3.32)}$ in M3, thus defining a negatively charged electrostatic microdomain within the binding-site crevice of the D2 receptor that would attract cationic ligands toward M2−M3 (see Figure 6B for a projection on the plane). The fourth acidic residue $Asp80^{(2.50)}$ is relatively far away from the other three acidic residues and, thus, belongs to a different motif within the receptor.

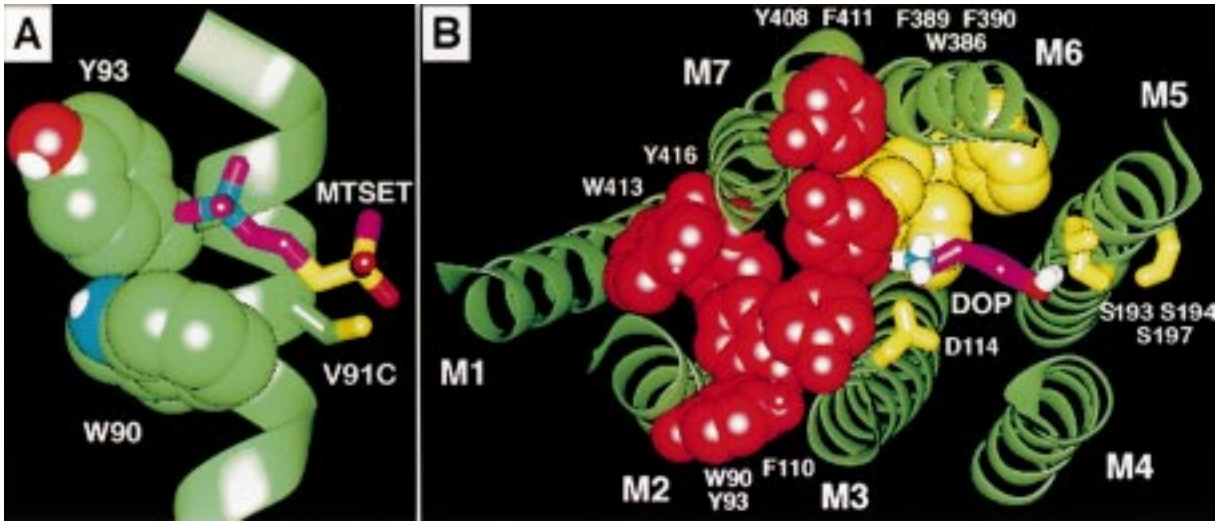

FIGURE 6: An aromatic microdomain in the binding-site crevice of the D2 receptor. (A) Molecular models of M2 and MTSET (liquorize) showing the favorable interaction of the quaternary ammonium group of MTSET with the aromatic moieties of W90 and Y93 (van der Waals), which positions the disulfide moiety of MTSET in the right geometry for a nucleophilic attack by the thiolate of the substituted Cys at position 91 (liquorize), thus facilitating the reaction. (B) Dopamine (purple, liquorize) is shown binding between M3, M5, and M6. Residues in these helices previously proposed to contact dopamine (Asp114 in M3, Ser193, Ser194, and Ser197 in M5, and Trp386, Phe389, and Phe390 in M6) are shown in yellow. Enhanced reactivity of MTSET at several positions in M2 (this work), M6 (*10*) and M7 (*9*) identifies a dense cluster of aromatic residues contained within M2, M3, and M7, shown by van der Waals representations in red. The three-dimensional motif defined by this aromatic microdomain is positioned next to the dopamine binding site at the level of the protonated amine. All these aromatic residues shown in red were accessible in the binding-site crevice, except Tyr93 in M2, the aromatic moiety of which is significantly longer than the substituted Cys and thus may reach toward the receptor interior at the level of the M2−M3 interface.

to be close to Asp108$^{(3.26)}$ and to Asp114$^{(3.32)}$ in M3 (Figure 5B). These three residues generate a negative electrostatic potential that likely attracts and orients positively charged ligands to the M2−M3 portion of the binding-site crevice, thereby facilitating the direct interaction of the protonated amine of dopamine with Asp114.

The fourth acidic residue accessible in the binding-site crevice is Asp80. This residue, 15 amino acids away from Glu95, is likely to be too far from the three acidic residues at the top of M2 and M3 to be part of the same structural motif (Figure 5B; see below)

Aromatic Microdomain within M2, M3, and M7. Another factor that may contribute to the enhanced rate of reaction of MTSET with V91C and with V94C is the known affinity of hydrophobic cations for aromatic moieties. We have observed such an enhanced rate of reaction of MTSET with T412C in M7 (*9*) and with F389C and F390C in M6 (*10*), and we have noted that the specific increase may be the result of an interaction of the aromatic side chains of nearby residues with the hydrophobic quaternary ammonium group of MTSET (*33*), which could attract the reagent and favor the reaction of MTSET at these positions. This proposed mechanism is illustrated in Figure 6A: the favorable interaction of the quaternary ammonium group of MTSET with the aromatic moieties of Trp90 and Tyr93 positions the disulfide moiety of MTSET in the right geometry for a nucleophilic attack by the thiolate of the substituted Cys at position 91, thus facilitating the reaction. A similar affinity-driven attraction and reorientation of MTSET to react with V94C could be modeled (data not shown). Although the substituted Cys at Tyr93 was not accessible to the MTS reagents, the longer aromatic moiety of the native Tyr may extend sufficiently toward the receptor interior at the level of the M2−M3 interface to interact favorably with Trp90 and other accessible aromatic side chains (Figure 6B). Figure 6B illustrates our results in the structural context of the transmembrane domain of the D2 receptor, modeled following the seven helical template of bovine rhodopsin derived from electron microscopy (*29*, *30*). Notable is the presence of a dense cluster of aromatic side chains contained within M2, M3, and M7 (in red), that define a structural microdomain (*34*) within the D2 receptor. Except for Tyr93 (see above), all of these aromatic residues from M2, M3, and M7, shown in red in Figure 6B, were found to be accessible in this and our previous studies (*7*, *9*).

The increased MTSET reactivity seen at particular substituted Cys in M6 and M7, which we rationalized based on ET-aromatic interactions at the level of a single helix similar to Figure 6A (see Figure 7 in ref *9*, and Figure 7 in ref *10*), can now be understood within the context of the aromatic microdomain within M2, M3, and M7 (Figure 6B), which includes and expands the previously proposed ET−aromatic interactions.

The functional role of this newly identified aromatic microdomain contained within M2, M3, and M7 of the D2 receptor is not yet known. Its positioning next to the dopamine binding site at the level of the protonated amine (Figure 6B), however, suggests a role in ligand selectivity. This hypothesis is supported by the observation that several of these aromatic side chains are subtype selective. For instance, bulky substituents arising from the protonated amine would be expected to clash with this aromatic microdomain in the D2 receptor and, yet, fit in another subtype, such as the D4 receptor, which lacks several of these aromatic residues. We have recently corroborated this hypothesis by an extensive mutagenesis approach exchanging this M2-M3-M7 microdomain between the D2 and the D4 receptors (Simpson et al., in preparation).

Role of Asp80. The highly conserved Asp80$^{(2.50)}$ has been implicated in the binding of sodium (*15*, *16*), and its mutation

has been found to affect agonist binding to a great number of GPCRs (*12*, *15*, *16*, *35*, *36*). Our results support an indirect role of Asp80 in agonist binding. The rate of reaction of MTSEA is quite slow at D80C, more than 10 times slower than its reaction with Cys118 in M3, a residue one helical turn below Asp114, which is directly involved in ligand binding (*37*). The slow rate seen at D80C is consistent with that observed deep in the binding-site crevice of the other membrane-spanning segments and is not consistent with ready access of agonist to a binding site at this position. Moreover, Asp114 is likely to be in the second helical turn of M3, while Asp80 is likely to be in the fifth helical turn of M2, making the distance between them (>16 Å) too great to be spanned by a catecholamine agonist.

Mutation of Asp80 led to a loss of high-affinity agonist binding and severely impaired inhibition of adenylyl cyclase by D2 receptors (*16*). Mutation of Asp80 also decreased the regulation of the affinity of D2 receptors for agonists and for substituted benzamide antagonists (such as sulpiride) by sodium and pH. Thus, it is likely that Asp80 is necessary for the receptor to adopt its active conformation. While we observed a 7-fold decrease in the affinity of D80C for sulpiride, its affinity for *N*-methylspiperone, which is not sodium dependent, was increased nearly 3-fold. A receptor that cannot achieve the active conformation would be expected to gain affinity for an inverse agonist, which binds with higher affinity to the inactive state of the receptor. Consistent with this prediction, recent work has suggested that a number of antagonists, including spiperone, are inverse agonists at the D2 receptor (*38*, *39*).

ACKNOWLEDGMENT

We thank Drs. Olivier Civelli, Brian Kobilka, and Steve Rees for the human D2 receptor cDNA, the epitope-tagged β2 adrenergic receptor cDNA, and the pcin4 vector, respectively. We thank Thomas Livelli for the HEK 293 and the 293-TSA cells and for valuable advice. We thank Myles Akabas, Arthur Karlin, and Harel Weinstein for valuable discussion and for comments on this manuscript.

REFERENCES

1. Civelli, O., Bunzow, J. R., Grandy, D. K., Zhou, Q. Y., and Van Tol, H. H. (1991) *Eur. J. Pharmacol. 207* (4), 277−86.
2. Strader, C. D., Fong, T. M., Tota, M. R., Underwood, D., and Dixon, R. A. (1994) *Annu. Rev. Biochem. 63*, 101−32.
3. Oprian, D. D. (1992) *J. Bioenerg. Biomembr. 24* (2), 211−7.
4. Akabas, M. H., Kaufmann, C., Archdeacon, P., and Karlin, A. (1994) *Neuron 13*, 919−927.
5. Akabas, M. H., Stauffer, D. A., Xu, M., and Karlin, A. (1992) *Science 258* (5080), 307−10.
6. Javitch, J. A., Li, X., Kaback, J., and Karlin, A. (1994) *Proc. Natl. Acad. Sci. U.S.A. 91* (22), 10355−9.
7. Javitch, J. A., Fu, D., Chen, J., and Karlin, A. (1995) *Neuron 14* (4), 825−31.
8. Javitch, J. A., Fu, D., and Chen, J. (1995) *Biochemistry 34* (50), 16433−9.
9. Fu, D., Ballesteros, J. A., Weinstein, H., Chen, J., and Javitch, J. A. (1996) *Biochemistry 35* (35), 11278−85.
10. Javitch, J. A., Ballesteros, J. A., Weinstein, H., and Chen, J. (1998) *Biochemistry 37* (4), 998−1006.
11. Stauffer, D. A., and Karlin, A. (1994) *Biochemistry 33* (22), 6840−9.
12. van Rhee, A. M., and Jacobson, K. A. (1996) *Drug Dev. Res. 37*, 1−38.
13. Hamaguchi, N., True, T. A., Saussy, D. L., Jr., and Jeffs, P. W. (1996) *Biochemistry 35* (45), 14312−7.
14. Dohlman, H. G., Caron, M. G., Strader, C. D., Amlaiky, N., and Lefkowitz, R. J. (1988) *Biochemistry 27* (6), 1813−7.
15. Horstman, D. A., Brandon, S., Wilson, A. L., Guyer, C. A., Cragoe, E. J. J., and Limbird, L. E. (1990) *J. Biol. Chem. 265* (35), 21590−5.
16. Neve, K. A., Cox, B. A., Henningsen, R. A., Spanoyannis, A., and Neve, R. L. (1991) *Mol. Pharmacol. 39* (6), 733−9.
17. Zhou, W., Flanagan, C., Ballesteros, J. A., Konvicka, K., Davidson, J. S., Weinstein, H., Millar, R. P., and Sealfon, S. C. (1994) *Mol. Pharmacol. 45*, 165−170.
18. Sealfon, S. C., Chi, L., Ebersole, B. J., Rodic, V., Zhang, D., Ballesteros, J. A., and Weinstein, H. (1995) *J. Biol. Chem. 270* (28), 16683−8 (issn, 0021−9258).
19. Ballesteros, J. A., and Weinstein, H. (1995) *Methods Neurosci. 25*, 366−428.
20. Rees, S., Coote, J., Stables, J., Goodson, S., Harris, S., and Lee, M. G. (1996) *BioTechniques 20*, 102−110.
21. Roberts, D. D., Lewis, S. D., Ballou, D. P., Olson, S. T., and Shafer, J. A. (1986) *Biochemistry 25* (19), 5595−601.
22. Dohlman, H. G., Caron, M. G., Strader, C. D., Amlaiky, N., and Lefkowitz, R. J. (1988) *Biochemistry 27* (6), 1813−7.
23. Barlow, D. J., and Thornton, J. M. (1988) *J. Mol. Biol. 201* (3), 601−19.
24. Ballesteros, J. A., and Weinstein, H. (1992) *Biophys. J. 62* (1), 107−9.
25. Sansom, M. S. (1992) *Protein Eng. 5* (1), 53−60.
26. Williams, K. A., and Deber, C. M. (1991) *Biochemistry 30* (37), 8919−23.
27. Woolfson, D. N., Mortishire, S. R. J., and Williams, D. H. (1991) *Biochem. Biophys. Res. Commun. 175* (3), 733−7.
28. Javitch, J. A., Fu, D., and Chen, J. (1996) *Mol. Pharmacol. 49* (4), 692−8.
29. Unger, V. M., Hargrave, P. A., Baldwin, J. M., and Schertler, G. F. (1997) *Nature 389* (6647), 203−6.
30. Schertler, G. F. X., and Hargrave, P. A. (1995) *Proc. Natl. Acad. Sci. U.S.A. 92*, 11578−11582.
31. Baldwin, J. M. (1993) *EMBO J. 12* (4), 1693−703.
32. Elling, C. E., and Schwartz, T. W. (1996) *EMBO J. 15* (22), 6213−9.
33. Dougherty, D. A. (1996) *Science 271* (5246), 163−168.
34. Ballesteros, J., Kitanovic, S., Guarnieri, F., Davies, P., Fromme, B. J., Konvicka, K., Chi, L., Millar, R. P., Davidson, J. S., Weinstein, H., and Sealfon, S. C. (1998) *J. Biol. Chem. 273* (17), 10445−53.
35. Strader, C. D., Sigal, I. S., Register, R. B., Candelore, M. R., Rands, E., and Dixon, R. A. (1987) *Proc. Natl. Acad. Sci. U.S.A. 84* (13), 4384−8.
36. Strader, C. D., Sigal, I. S., Candelore, M. R., Rands, E., Hill, W. S., and Dixon, R. A. (1988) *J. Biol. Chem. 263* (21), 10267−71.
37. Strader, C. D., Gaffney, T., Sugg, E. E., Candelore, M. R., Keys, R., Patchett, A. A., and Dixon, R. A. (1991) *J. Biol. Chem. 266* (1), 5−8.
38. Hall, D. A., and Strange, P. G. (1997) *Br. J. Pharmacol. 121* (4), 731−6.
39. Kozell, L. B., and Neve, K. A. (1997) *Mol. Pharmacol. 52* (6), 1137−49.
40. Cheng, Y., and Prusoff, W. H. (1973) *Biochem. Pharmacol. 22* (23), 3099−108.

BI9905314